J. Membrane Biol. 163, 235–245 (1998)

The Journal of
Membrane
Biology

The Effect of Electrical Deformation Forces on the Electropermeabilization of Erythrocyte Membranes in Low- and High-Conductivity Media

V.L. Sukhorukov, H. Mussauer, U. Zimmermann
Lehrstuhl für Biotechnologie, Biozentrum, Universität Würzburg, Am Hubland, D-97074 Würzburg, Germany

Received: 12 December 1997/Revised: 13 March 1998

Abstract. Electrical breakdown of erythrocytes induces hemoglobin release which increases markedly with decreasing conductivity of the pulse medium. This effect presumably results from the transient, conductivity-dependent deformation forces (elongation or compression) on the cell caused by Maxwell stress. The deformation force is exerted on the plasma membrane of the cell, which can be viewed as a transient dipole induced by an applied DC electric field pulse. The induced dipole arises from the free charges that accumulate at the cell interfaces via the Maxwell-Wagner polarization mechanism. The polarization response of erythrocytes to a DC field pulse was estimated from the experimental data obtained by using two complementary frequency-domain techniques. The response is very rapid, due to the highly conductive cytosol. Measurements of the electrorotation and electrodeformation spectra over a wide conductivity range yielded the information and data required for the calculation of the deformation force as a function of frequency and external conductivity and for the calculation of the transient development of the deformation forces during the application of a DC-field pulse. These calculations showed that (i) electric force precedes and accompanies membrane charging (up to the breakdown voltage) and (ii) that under low-conductivity conditions, the electric stretching force contributes significantly to the enlargement of ''electroleaks'' in the plasma membrane generated by electric breakdown.

Key words: Erythrocytes — Medium conductivity — Electropermeabilization — Electrodeformation — Electrorotation

Correspondence to: U. Zimmermann

Introduction

Electropermeabilization allows the introduction of membrane-impermeable xenomolecules (such as dyes, drugs, hormones, proteins, plasmids, etc.) into living cells as well as the controlled release of intracellular substances [14, 18, 24, 25, 39]. The field technique is based on the reversible electric breakdown of cell membranes [22, 38]. A single (or a train of) external exponentially decaying electric field pulse(s) of a few kV cm^{-1} field strength and of several microseconds duration is required to induce reversible breakdown of the plasma membrane. Breakdown occurs when the transmembrane potential exceeds 1 V at room temperature. The degree of membrane permeabilization upon breakdown depends critically on the conductivity of the pulse medium (and other parameters [20, 25, 39]). This has been demonstrated recently by the injection of propidium iodide into mammalian cells [6]. The forces which are responsible for the enlargement of the ''electroleaks'' under low-conductivity conditions are unknown.

A parameter which is usually not taken into account in the theory of electropermeabilization of cell membranes is the transient deformation force exerted on the membrane, i.e., on the electric dipole induced within the cell by the high-intensity electric field pulse. The induced dipole arises from the free charges that accumulate at the two cell interfaces, i.e., at the inner and outer boundaries of the plasma membrane. This phenomenon is known as the Maxwell-Wagner interfacial polarization [12, 23, 30]. The resulting deformation force is caused by the Maxwell stresses applied to the cell interfaces [5, 19, 29, 31, 36]. The polarity of this force depends on the orientation of the induced dipole (i.e., of the interfacial charges) which, in turn, is determined by the effective polarizability of cells relative to the suspending media. Due to the layered structure of the cells, the magnitude

and polarity of the force can vary with time in a complicated manner [12, 23].

Electrodeformation can explain the observed dependence of electropermeabilization on medium conductivity because (i) the magnitude of the generated dipole and the deformation force are conductivity-dependent and (ii) they occur in a few nanoseconds (*see* below) in contrast to electric membrane breakdown which occurs in the microsecond range once the membrane is charged to the critical voltage of 1 V [39]. Therefore, cell deformation forces (depending on medium conductivity) can precede and accompany the reversible electric breakdown and the subsequent permeabilization of the plasma membrane. However, the development of deformation forces during the electropermeabilization process of the cells and their effect on the high-permeability state of the membrane has not yet been considered, presumably because of the lack of the relevant electric data and their relation to the induced-dipole moment, **μ**.

In this communication, we present theoretical and experimental evidence that these data can be extracted from measurements of the conductivity dependence of the electrorotation and electrodeformation spectra of cells in time-varying (alternating current or rotating) fields. In such fields, the electrodeformation and, particularly, the electrorotation responses of cells can be measured quite accurately over a very wide frequency range at various conductivities of the media [1, 5, 12, 17, 26, 34, 35]. The frequency results can easily be transformed into the time domain using standard mathematical methods [7]. Thus, the magnitude and the time course of the electrodeformation force upon pulse administration can be derived from complementary measurements of cell deformation and rotation induced by alternating current or rotating fields.

Measurements were performed with human erythrocytes. Due to their biconcave shape *iso-volume* deformation could be measured quite easily and accurately [9]. As an indicator of the conductivity-dependent electropermeabilization process the field-induced hemoglobin release from the cells was used.

It is demonstrated that (i) the hemoglobin release increased with decreasing medium conductivity as expected in the light of the uptake studies of xenomolecules [6] and (ii) that the transient stretching force on the cell membrane due to the electric polarization of the cells accounts predominantly for the observed effects of the external conductivity on electropermeabilization. This latter conclusion could be drawn from the finding that the dependence of hemoglobin release on medium conductivity found experimentally agreed very well with the calculation of the conductivity-dependent temporal polarization $\mu(t)$ (by using the data extracted from the frequency-domain measurements).

Theoretical Considerations

For modelling the electrodeformation and electrorotation spectra, erythrocytes (suspended in an aqueous medium with permittivity $\varepsilon_e = 80\ \varepsilon_0$, $F\ m^{-1}$ and conductivity σ_e, $S\ m^{-1}$) are approximated by the single-shell spherical model, *i.e.*, they are viewed as conductive spheres of radius a (with a conductivity σ_i and permittivity ε_i) surrounded by a shell of thickness *d*. The shell corresponds to the plasma membrane which has a conductivity σ_m, a permittivity ε_m, an area-specific capacitance $C_m = \varepsilon_m/d$ ($F\ m^{-2}$) and an area-specific conductance $G_m = \sigma_m/d$ ($S\ m^{-2}$). It is assumed that the conductivities, permittivities, C_m and G_m are independent of the frequency of the applied external field.

Theoretical Relationships Between Electrodeformation, Dielectrophoresis and Electrorotation Spectra

Fundamentals

Time varying electric fields (and also DC-field pulses) generate a dipole within a suspended cell [21, 23, 33]. The induced dipole arises from the free charges that accumulate at the interface(s) of the cell if its electrical properties differ from those of the suspending medium.

The induced-dipole moment **μ** is proportional to the applied-field strength, ***E***, and to the effective polarizability of the cell *U* relative to the suspending medium [12, 15]:

$$\boldsymbol{\mu} = 4\pi\varepsilon_e a^3 \cdot U \cdot \boldsymbol{E} \tag{1}$$

Eq. 1 states that the effective polarizability of the cell U determines the induced-dipole moment and, therefore, the mechanical forces, pressures and torques on a cell due to the interaction of the induced dipole **μ** with the external field ***E*.**

In the presence of high-frequency (kHz-MHz) sinusoidal or rotating electric fields, the polarizability of a cell is a complex function of the field frequency. $U = U^*(f)$ is known as the Clausius-Mosotti function. As shown elsewhere [28] the following equations for the complex polarizability and permittivity of a single-shelled spherical particle (denoted with the subscript ''*c*'') can be derived:

$$U^*(f) = \frac{\varepsilon_C^* - \varepsilon_e^*}{\varepsilon_C^* + 2\varepsilon_e^*} \tag{2}$$

$$\varepsilon_C^* = \frac{aC_m^* \cdot \varepsilon_i^*}{aC_m^* + \varepsilon_i^*} \tag{3}$$

where ε^* is the complex permittivity defined as: $\varepsilon^* = \varepsilon - j\sigma/\omega$; C_m^* is the complex membrane capacitance per unit area given by: $C_m^* = C_m - j\, G_m/\omega$; $j = (-1)^{1/2}$; $\omega = 2\pi f$ is the radian field frequency.

The dielectrophoretic force [3, 12, 23, 27, 33] and also the electric deformation force [5, 8, 19, 29, 36] are proportional to the real part, $Re(U^*)$, of the Clausius-Mosotti function, whereas the imaginary part, $Im(U^*)$, determines electrorotation [2, 11, 12, 15, 23, 26, 27]. This demonstrates that electrodeformation (as well as dielectrophoresis, a term used to signify cell movement induced by a nonuniform field) and electrorotation are theoretically related and also intimately related in practice if the correct model is being used [12].

On the line of the arguments given in [8, 29] it can be shown that, for relatively small cell deformations, the elastic stain ($\Delta l/l_0$) depends on the cell polarizability U^* as follows:

$$\frac{\Delta l}{l_0} = \alpha E^2 Re(U^*) \tag{4}$$

where the scaling factor α accounts for the elastic properties of the erythrocyte (which are determined mainly by the cytoskeleton [4]). ($\Delta l/l_0$) is the measurable parameter. The change (Δl) in length and the original length (l_0) are in the direction parallel to the field. Positive and negative values of the strain indicate cell elongation and compression, respectively.

The frequency dependence of the dielectrophoretic force on a cell (F_{DEP}) is given by [3, 12, 15, 23, 27]:

$$F_{DEP} = 2\pi a^3 \varepsilon_e\, Re(U^*) \nabla E^2 \tag{5}$$

where ∇ denotes the del vector operator. Positive and negative values of the dielectrophoretic force indicate cell attraction to and repelling from the electrodes, respectively. It must be noted that the normalized electrodeformation and dielectrophoresis spectra are identical because they are determined completely by the real part of the Clausius-Mosotti factor. However, in contrast to electrodeformation, the dielectrophoretic force vanishes in an uniform electric field.

As shown elsewhere [2, 12] the steady-state rotation speed (Ω) of a cell in a rotating field is given by:

$$\Omega = -\varepsilon_e E^2\, Im(U^*)/2\eta \tag{6}$$

where η is the dynamic viscosity of the medium.

Spectra

Theoretical plots of the real and imaginary components of $U^*(f)$ as functions of the applied field frequency are shown in Figs. 1*A* and *B*. The frequency spectra of

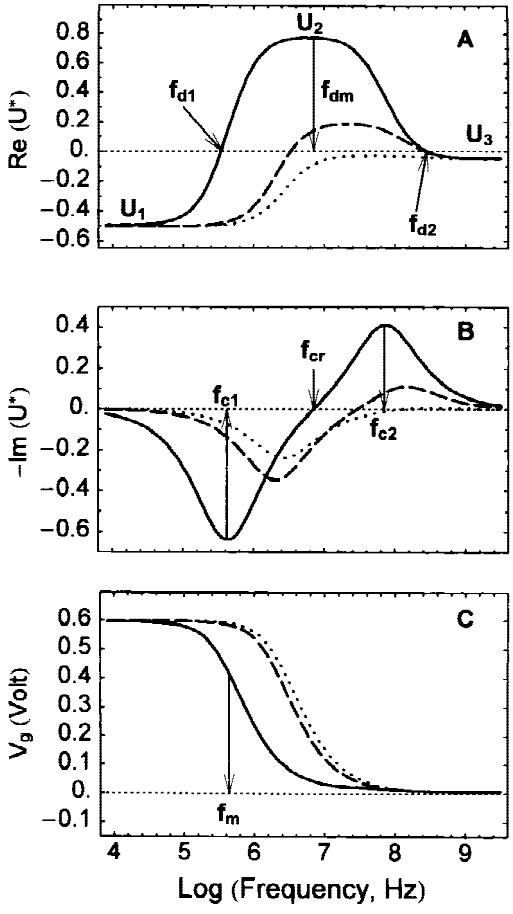

Fig. 1. Theoretical plots of the real (*A*) and imaginary (*B*) parts of the Clausius-Mosotti function U^* as well as of the induced membrane potential V_g (*C*) *vs.* the logarithm of the field frequency using Eqs. 2 and 3 and Eq. 8, respectively. The spectra of $Re(U^*)$ and $Im(U^*)$ as well as the dependence of V_g on frequency were calculated for three conductivities of the suspending medium, σ_e, 0.5 mS cm^{-1} (solid curves), 4.5 mS cm^{-1} (dashed curves) and 8.5 mS cm^{-1} (dotted curves); the erythrocyte was approximated by the single-shell model (*see* text) by using the following parameters: $a = 4$ μm, $C_m = 0.8$ μF cm^{-2}, $G_m = 10$ mS cm^{-2}, $\varepsilon_i = 70\ \varepsilon_0$, $\sigma_i = 8$ mS cm^{-1}, $\varepsilon_e = 80\ \varepsilon_0$; the field strength was assumed to be 10^3 V cm^{-1}. f_{d1} and f_{d2} are the crossover frequencies of dielectrophoresis, f_{c1} and f_{c2} are the peak-frequencies of anti-field and co-field electrorotation, f_m is the characteristic frequency of membrane charging-related reciprocal of the relaxation time (Eq. 9). U_1, U_2 and U_3 in (*A*) represent $Re(U^*)$ for the frequency ranges (at $f \ll f_{d1}$, at $f_{dm} = f_{cr}$ and at $f \gg f_{d2}$, respectively), where $Im(U)$ in (*B*) is close or equal to zero (Eqs. 7 a–c). For further explanations, *see* text.

$Re(U^*)$ and $Im(U^*)$ were calculated by using Eqs. 2 and 3 and by selecting appropriate parameters for a, C_m, G_m, σ_i and ε_i, *see* legend to Fig. 1). Calculations were made for three different specific conductivities of the suspending medium. In the case of $\sigma_e = 0.5$ mS cm^{-1} and 4.5 mS cm^{-1} the external specific conductivity was below and in the case of $\sigma_e = 8.5$ mS cm^{-1} above the specific internal conductivity σ_i.

It is obvious from Fig. 1*B* that the electrorotation spectrum consists of a negative (anti-field) and a positive (co-field) peaks centered at frequencies f_{c1} and f_{c2}, respectively, provided that $\sigma_i > \sigma_e$ (solid and dashed curves in Fig. 1*A* and *B*). These frequencies are close to the crossover frequencies f_{d1} and f_{d2} of the electrodeformation (dielectrophoresis) spectrum in Fig. 1*A*.

For $\sigma_i > \sigma_e$, cells exhibit positive dielectrophoresis (*i.e.*, attraction to the electrodes) between f_{d1} and f_{d2}. In this frequency range, positive deformation of the cells (that is elongation parallel to the field lines) occurs. The frequency of maximum cell elongation (and of positive dielectrophoresis) f_{dm} coincides with the crossover frequency f_{cr} of the electrorotation spectrum. For frequencies below f_{d1}, cells show negative dielectrophoresis associated with cell compression in relation to the field lines. Above f_{d2}, the cells remain freely suspended and not deformed between the electrodes (*see* below).

As indicated in Fig. 1*A* and *B*, f_{c1} and f_{d1} shift towards higher frequencies with increasing conductivity of the medium, whereas f_{c2} and f_{d2} are less conductivity-dependent. Simultaneously, the rotation speed and deformation (as well as positive dielectrophoresis) between f_{d1} and f_{d2} decrease considerably with increase in conductivity. For $\sigma_i < \sigma_e$ (dotted curves in Fig. 1*A* and *B*), the co-field rotation peak [12] disappears and negative dielectrophoresis together with cell compression parallel to the field lines occur over the whole frequency range.

This dependency of the deformation- and dielectrophoresis-forces of the cells on the specific external conductivities becomes particularly evident if the Clausius-Mosotti function is considered for frequency ranges where the imaginary part approaches or is equal to zero (U at $f \gg f_{d2}$, U at $f \ll f_{d1}$ and U at the frequency indicated in Fig. 1*B* by $f_{cr} = f_{dm}$). Under these conditions, which are of practical use (*see* below), $U^*(f)$ becomes real and the following simplified equations hold [15, 23]:

$$U(f) = \begin{cases} U_3 = \dfrac{\varepsilon_i - \varepsilon_e}{\varepsilon_i + 2\varepsilon_e}, & f \gg f_{d2}, \\ U_2 = \dfrac{\sigma_i - \sigma_e}{\sigma_i + 2\sigma_e}, & f = f_{cr} = f_{dm}, \\ U_1 = \dfrac{a \cdot G_m(\sigma_i - \sigma_e) - \sigma_i\sigma_e}{a \cdot G_m(\sigma_i + 2\sigma_e) + 2\sigma_i\sigma_e}, & f \ll f_{d1}, \end{cases} \quad (7abc)$$

Using appropriate values of the cellular and membrane parameters it can be easily shown (Fig. 1*A*) that U_1 is nearly independent of the specific external conductivity. U_1 assumes negative values, that means cell compression in the direction parallel to the field lines and negative dielectrophoresis occur in the low frequency range ($f < f_{d1}$). Similarly, since ε_i is close to ε_e the polarization and the electric deformation force are negligible in the high frequency range ($f > f_{d2}$). However, inspection of Eq. 7*b* shows that in the intermediate frequency range (between f_{d1} and f_{d2}) the electric deformation force generated by the Maxwell stresses depends strongly on the external specific conductivity. If $\sigma_e < \sigma_i$ the force leads to cell elongation in field direction. In contrast, if $\sigma_e > \sigma_i$, U_2 becomes negative and, in turn, cell compression parallel to the field line occurs. In the special case of $\sigma_e = \sigma_i$ (not shown in Fig. 1*A*) the force disappears.

Membrane Charging in AC-Fields

When a sinusoidal electric field is applied, the induced membrane potential V_g at the cell pole facing the electrodes is given by the following Eq. [21]:

$$V_g = \frac{1.5 \cdot a \cdot E}{\sqrt{1 + (\omega\tau_m)^2}} \quad (8)$$

with the relaxation time constant of the plasma membrane polarization τ_m [22]:

$$\tau_m = aC_m\left(\frac{1}{\sigma_i} + \frac{1}{2\sigma_e}\right) \quad (9)$$

A plot of the generated membrane potential V_g *vs.* frequency for the three specific external conductivities of Fig. 1*A* and *B* (corresponding to relaxation times of 0.36, 0.08 and 0.06 μsec at 0.5, 4.5 and 8.5 mS cm^{-1}, respectively) is given in Fig. 1*C*. It is evident that V_g decreases continuously above a frequency f_m which is equal to the reciprocal relaxation time constant ($f_m = (2\pi\tau_m)^{-1}$) and close to the cross-over frequency f_{d1} of the deformation spectra. Similarly, the ''cutoff'' frequency f_m is shifted towards higher frequencies with increasing conductivity of the medium (0.44, 2 and 2.7 MHz for 0.5, 4.5 and 8.5 mS cm^{-1}, respectively). Comparison of Fig. 1*A* with Fig. 1*C* also shows that, in the frequency range of positive dielectrophoresis and deformation, the induced membrane potential is relatively small (due to the ''short-circuit'' of the plasma membrane; *see also* Fig. 2*B*). Maximum membrane charging (and thus AC-field-induced breakdown) is achieved only in the low frequency range $f < f_{d1}$ where negative dielectrophoresis and compression occurs.

The foregoing considerations are illustrated in Fig. 2 for the case of $\sigma_e < \sigma_i$. The field distribution around a single-shelled cell (Fig. 2, left-hand diagrams) was calculated for the three frequency ranges by solving the

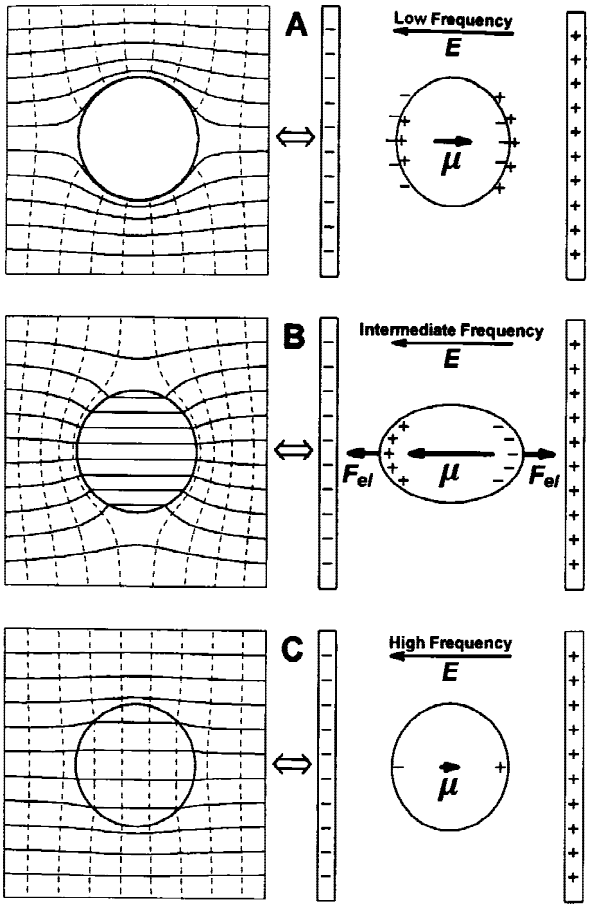

Fig. 2. The diagrams show the electric field distributions (left) and the corresponding induced-dipole moments, **μ,** within a spherical cell (right). The field distributions (solid lines; equipotential lines are indicated by dashed lines) and the dipole moments were calculated by using the Laplace equation [12, 23] and Eq. 1, respectively for a *low-conductivity* solution ($\sigma_e = 0.5$ mS cm^{-1}; $\sigma_i > \sigma_e$, $\varepsilon_i < \varepsilon_e$ and $\sigma_m \ll \sigma_e$). In the low- and high-frequency regions (*A* and *C*), the induced dipoles (μ) are anti-parallel to the applied field *E*, whereas at the intermediate frequencies (*B*) the dipole is oriented in the direction parallel to the field. The diagram *B* (right) shows that interaction of the external field *E* with the induced interfacial charges leads to the occurrence of elongation forces (F_{el}). For further explanation, *see* text.

Laplace equation (for details *see* [22]). The corresponding induced-dipole moments **μ** and the relevant induced interfacial charges are shown schematically (Fig. 2, right-hand diagrams). It is evident that the dipole moment is anti-parallel to the field ***E*** in the low frequency range (resulting in compression, Fig. 2*A*), but parallel to the external field in the intermediate frequency range (resulting in elongation, Fig. 2*B*). In this case, the membrane is ''short-circuited'' and the field lines pass through the cell interior: the cytosolic conductivity is the main determinant of the deformation response (as can be also seen from Eq. 7*b*). In the high frequency range (Fig. 2*C*), the dipole is small or even zero.

Relaxation Times of Cytosolic Polarization and Membrane Charging in DC-Pulse Fields

In response to an applied DC electric field ***E,*** the generated voltage across the plasma membrane is given by [38]:

$$V_g(t) = 1.5 \cdot a \cdot E \cdot (1 - \exp(-t/\tau_m)) \quad (10)$$

whereby τ_m is given by Eq. 9. Plots of the induced membrane potentials for the three external specific conductivities given in Fig. 1*C* (corresponding to $\tau_m = 0.36$, 0.08 and 0.06 μsec for solid, dashed and dotted lines, respectively) yield the curves shown in Fig. 3*A.*

During a DC-field pulse, the magnitude and the direction of the induced dipole moment **μ** is given first by U_3, then by U_2 and finally by U_1. This means that, after application of a DC-field pulse, transitions from cell compression to cell elongation force can occur provided that the pulse duration is long enough. In Fig. 3*B* the temporal polarization response of cell $U(t)$ is calculated for the three external specific conductivities of Fig. 1 by using appropriate values for the various parameters of the erythrocyte cell (*see* above) and by taking into account that the relaxation time of the cytosol polarization given by [23, 30]:

$$\tau_i = \frac{\varepsilon_i + 2\varepsilon_e}{\sigma_i + 2\sigma_e} \quad (11)$$

It is obvious that in the case of $\sigma_e < \sigma_i$ (solid and dashed curves in Fig. 3*B*) the elongation force reaches its maximum value about 1 nsec after pulse administration. This is much faster than the charging process of the membrane given in Fig. 3*A*. If $\sigma_e > \sigma_i$, the elongation force does not appear (dotted curve in Fig. 3*B*). Note that the theoretical plots of V_g as function of time (Fig. 3*A*) were calculated by assuming the external field strength $E = 1$ kV cm^{-1}, which is not sufficient to induce the membrane breakdown. However, the application of the field strength of 4 kV cm^{-1}, which was used in the electrohemolysis experiments (*see below* Fig. 4), will induce breakdown of the membrane (breakdown voltage $V_c = 1$ V) within $t_{1V} = 0.19$ μsec ($\sigma_e = 0.5$ mS cm^{-1}, $\tau_m = 0.36$ μsec, $a = 4$ μ*m*, $E = 4$ kV cm^{-1}, $t_{1V} = -\tau_m 1n(1 - V_C/1.5\,aE)$, *see* Eq. 10 and legends to Figs. 1 and 3). This means that electric breakdown of the cell membrane occurs within the time scale where the transient stretching force is still operational (i.e., $t < \tau_m = 0.36$ μsec). Therefore, we can conclude that (i) transient electrodeformation force (elongation/compression) precedes and accompanies membrane charging in response to pulsed DC electric field and that (ii) under conditions which leads to cell elongation (that is $\sigma_e < \sigma_i$, Fig. 2*B*) the transient stretching force can affect the enlargement

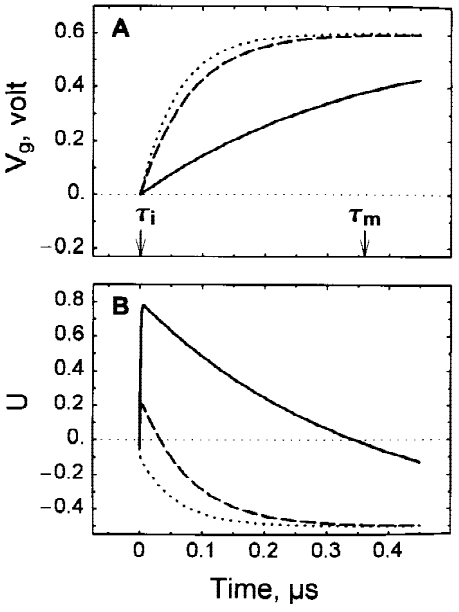

Fig. 3. Plot of the induced transmembrane potential V_g (*A*) and of the Clausius-Mosotti function U (*B*) as functions of time after administration of a DC-field pulse at time zero. The curves in the time domain (response to a step-function electric field) were evaluated from the frequency spectra shown in Fig. 1 by using standard transformation methods described elsewhere [7, 37]. Calculations were made for the same cell parameters, field strength and specific external conductivities as in Fig. 1. For $\sigma_e < \sigma_i$ maximum elongation stress (given by U) develops very rapidly compared to membrane charging and that elongation decreases with increasing external conductivity (solid and dashed lines). Elongation stress does not appear when σ_e exceeds σ_i (dotted line). The time constant of membrane polarization τ_m decreases with increasing σ_e. The arrows denoted by τ_i (Eq. 11) and τ_m (Eq. 9) indicate the time constants of the cytosolic polarization and the plasma membrane charging for $\sigma_e = 0.5$ mS cm^{-1}. (Note that the field strength of 1 kV cm^{-1} assumed for calculations of V_g (*A*) is not sufficient to induce the critical membrane voltage $V_C = 1$ V).

of the electroleaks generated at the membrane sites oriented in field direction.[1]

Materials and Methods

Electropermeabilization of Cells

Human blood samples were withdrawn from apparently healthy donors and used on the day of collection. The red blood cells (RBCs) were isolated and washed as described elsewhere [35]. The cells (10^8 cells per ml) were then kept in phosphate buffered saline (PBS, 136 mM NaCl, 10 mM KH_2PO_4, pH 6.5) at 4°C. 5–10 min before electropermeabilization, the cells were transferred into media of different conductivities (final density: $1–3 \cdot 10^6$ cells per ml). The conductivity was adjusted by addition of 4–65 mM KCl or NaCl. In some experiments 3–40 mM Na_2SO_4 were also used. The media were buffered to a pH of 6.5 by using 0.5–5 mM K_2HPO_4/KH_2PO_4. Iso-osmolality of the media (280 mosmol kg^{-1}) was achieved by the addition of appropriate amounts of inositol. Conductivity and osmolality of the solutions were measured by means of a conductometer (Knick GmbH, Berlin, Germany) and a cryoscopic osmometer (Osmomat 030, Gonotec GmbH, Berlin, Germany).

The cells were subjected to a single exponentially decaying pulse of 4 kV cm^{-1} strength and a decay time constant of 20 μsec (at 22–24°C) by using two commercial electroporators (the Biojet MI, Biomed, Theres, Germany and the Multiporator, Eppendorf, Hamburg, Germany). The field strength of 4 kV cm^{-1} is nearly a factor of 2 higher than the critical field strength required to reach the breakdown voltage at membrane sites located in field direction (assuming an average cell radius of 3–4 μm; *see* [32, 39]). The discharge chamber consisted of two flat stainless-steel electrodes (0.1–0.6 cm apart). The discharge process was monitored by means of a digital storage oscilloscope (Digitalscope SE571, BBC Goerz Metrawatt, Austria) connected to the electrodes (for details *see* [6]). 10 min after field application, the samples were centrifuged (650 × *g*, 5 min), and the absorption spectra of the supernatants in the wavelength range from 350 to 700 nm were measured by using a Perkin-Elmer Lambda 2 UV/VIS spectrophotometer. The 415 nm adsorbance of the samples was used to quantitate hemoglobin in the supernatants. Absorbance values for 100% hemoglobin release were obtained by the addition of saponin (0.2%; Merck No. 7695).

Electrorotation Experimentals

Erythrocytes were suspended in 280–300 mOsm inositol solution containing appropriate amounts of PBS to adjust the conductivity to 0.1–2.5 mS cm^{-1} (at 20–24°C). Electrorotation spectra were measured in a microstructured four-electrode chamber developed by G. Fuhr (Humboldt-University, Berlin, Germany). The microstructured chamber, which was made by semiconductor technology [12, 16], was arranged as a planar array of circular electrodes of 60 μm diameter, 1 μm thickness and 300 μm electrode spacing. The miniaturization and the associated improvement of heat-dissipating properties of the electrodes allowed the use of relatively low voltages and high-conductivity solutions. The electrodes were driven by four 90° phase-shifted, symmetrically rectangular signals from a computer-controlled pulse generator HP 8130A (Hewlett-Packard, Boeblingen, Germany) with 2–4 V_{PP} amplitude over the frequency range from 100 Hz to 150 MHz. The rotation spectra were normalized to the driving voltage of 3 V_{PP} in accordance with Eq. 6. The spectra were monitored using a Leica Metalux microscope equipped with a high-resolution CCD video camera (HR 480, aqua-tv, Kempten, Germany) connected through a S-VHS video-recorder (RTV-925 HIFI, Blaupunkt, Hildesheim, Germany) to a monitor (TC-1470, Panasonic, Matsushita, Japan).

The rotation spectra were fitted on the basis of the single-shell model (combination of Eqs. 2, 3 and 6) using the *Mathematica*® software [37]. The spectra were corrected by the scaling factor, χ ($\chi = \varepsilon_e E^2/2\eta$, *see* Eq. 6), that accounts for the poorly characterized local field strength and for the frictional force experienced by an individual cell [13].

Electrodeformation

Electrodeformation experiments were carried out using a microstructure that consisted of a planar array of 20 parallel interdigitated micro-

[1] Transient electrodeformation has to be distinguished from the deformation of erythrocytes upon application of a *constant* force. In this case the response time is of the order of 0.1–1 sec [9] (*see also* Results, Figs. 6–8).

electrodes. The electrode fingers (made of platinum) were 0.5 μm thick, 10 μm wide and 100 μm long. The gap between neighboring electrodes was 50 μm. The adjacent electrodes were driven by two 180° phase-shifted rectangular signals from the pulse generator HP 8130A (*see* above) with 1.0–9.6 V_{PP} amplitude over the frequency range from about 1 kHz to 300 MHz. For each experiment, 50–70 μl of cell suspension (about 3×10^5 cells ml^{-1}) was pipetted onto the microchamber and a coverslip was gently placed over its center. After cells had settled for about 3 min, a 2-MHz field of 0.1–0.2 kV cm^{-1} was applied for 5–10 sec to direct cells to the electrode edges by positive dielectrophoresis. The electrodeformation spectra were monitored by decreasing the field frequency in steps (5–10 frequency points per decade starting at 300 MHz) while the field strength was kept constant (1.6 kV cm^{-1}). The field strength dependence of the electrodeformation force was measured at a frequency of 2 MHz (*see* Results). The observation of the deformation response of the cells to the AC field was performed using an Olympus microscope (BX, Olympus, Hamburg, Germany) equipped with a high-resolution monochrome CCD camera (SSC-M370CE, Sony, Cologne, Germany). The video camera was connected to an IBM compatible personal computer equipped with a video digitizing board and an image capture software ''Screen Machine II'' (Fast Electronics, Munich, Germany). For each erythrocyte within a cell sample (usually 10–12 cells), its maximal original length (l_0, without field) and its maximal lengths (l, after field application) in the direction parallel to the field lines at various frequencies (or strengths) were determined using a commercial image measurement software ''SigmaScan'' (Jandel GmbH, Erkrath, Germany). The electrodeformation spectra, that is the relative deformation $(l - l_0)/l_0 = \Delta l/l_0$ (Eq. 4) as a function of the field frequency, were evaluated from the sequences of 20–30 images of the same cell sample. In separate experiments, the erythrocytes were photographed using a camera MPS 52 (Wild Leitz, Heerbrugg, Switzerland).

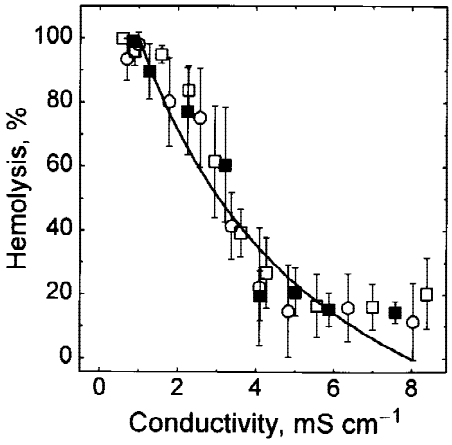

Fig. 4. The dependence of the electrohemolysis of human erythrocytes (in percentage) on medium conductivity. The cells were exposed to a single exponentially decaying pulse of 4 kV cm^{-1} strength and 20 μsec duration at 22–24°C. The conductivity of the isoosmolar pulse medium (280 mosmol kg^{-1}) was varied by addition of appropriate concentrations of KCl (open circles), NaCl (filled circles) and Na_2SO_4 (squares). The released hemoglobin was determined spectrophotometrically in the supernatant 10 min after field application. The datapoints are the means of 3–4 independent measurements; the bars represent the standard deviation. Note, that at a given medium conductivity the ionic strength of the Na_2SO_4-containing media (squares) was approximately twice as high as that of the corresponding KCl- or NaCl-containing media. The curve shows the theoretical relationship between the cytosolic polarization of the cell $U_2 = (\sigma_i - \sigma_e)/(\sigma_i + 2\sigma_e)$ (Eq. 7*b*) and the medium conductivity, σ_e (U_2 is normalized to its value at $\sigma_e = 1$ mS cm^{-1}. For further explanation, *see* text).

Results and Discussion

Effect of Medium Conductivity on the Electrohemolysis

Figure 4 shows the effect of the medium conductivity on the release of hemoglobin from electropermeabilized erythrocytes. It is obvious that the hemoglobin release decreased markedly with the increase of the medium conductivity up to a value of about 4 to 6 mS cm^{-1}. Beyond this value the release was low (about 5–15%) and more or less independent of the medium conductivity. In contrast, almost complete release of hemoglobin was observed at a very low conductivity (about 1 mS cm^{-1}). Figure 4 shows that, at a given pulse medium conductivity, the replacement of the K^+- and Cl^--ions by Na^+ and SO_4^{2-}-ions in the pulse medium had no influence on the coductivity-dependence of the field-mediated hemolysis. These findings are in agreement with the results observed recently for electrically induced incorporation of propidium iodide into mouse myeloma cells [6].

Transient stretching force acting on the plasma membrane of the erythrocytes upon application of the high-intensity DC-field pulse is presumably the reason for the conductivity-dependence of the hemoglobin release as suggested by the experiments in time-varying fields presented below.

Effect of Medium Conductivity on Electrorotation

Relevant data for fitting the deformation spectra of erythrocytes monitored in AC-fields were extracted from electrorotation spectra. As shown in the section ''Theoretical Considerations'' electrorotation and electrodeformation are complementary phenomena. The experimental setup used in this study for electrorotation allowed both anti- and co-field rotation peaks to be resolved and, therefore, the measurement of the frequency spectra of the induced dipole $\mu(f)$ could be performed up to a frequency of 150 MHz. This frequency range was large enough to achieve the accuracy required for the determination of the relevant membrane and cellular parameters (such as C_m, G_m, σ_i and ε_i) by fitting the experimental electrorotation spectra. In contrast, the measurements of the electrodeformation spectra were limited to only a very narrow frequency range between f_{d1} and f_{d2} (*see* below and Fig. 1*A*).

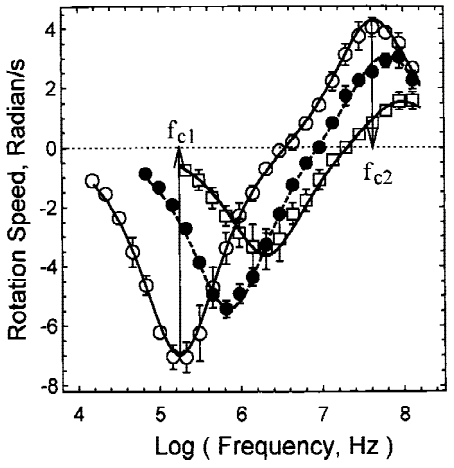

Fig. 5. Electrorotation spectra of human erythrocytes performed in media of different conductivities: $\sigma_e = 0.11$ mS cm^{-1} (open circles), $\sigma_e = 0.54$ mS cm^{-1} (filled circles) and $\sigma_e = 1.95$ mS cm^{-1} (squares). The curves show the best fits of the single-shell model (combination of Eqs. 2, 3 and 8) to the experimental data. The datapoints are the mean ± SD of 5–6 cells. For extraction of the relevant cellular parameters from the curves, *see* text.

Typical electrorotation spectra of erythrocytes measured at various external conductivities are shown in Fig. 5. As expected theoretically [12], the anti-field ''plasma-membrane'' rotation peak (f_{c1}) shifted with increasing conductivity towards higher frequencies. Fitting of the single-shell model to the experimental data in Fig. 5 yielded the following parameters: the area-specific membrane capacitance $C_m = 0.6$–0.65 μF cm^{-2}, the area-specific membrane conductance $G_m = 10$–50 mS cm^{-2} and the dielectric constant of the cytosol $\varepsilon_i = 80$–90. The value of the internal specific conductivity (σ_i) decreased with decreasing external conductivity (σ_e) and was found to be 8, 7 and 5.5 mS cm^{-1} at the external conductivities of 2, 0.54 and 0.11 mS cm^{-1}, respectively. The decrease of the internal conductivity in low-salinity media was obviously due to ion leakage from the erythrocytes [35].

AC-Field-Induced Deformation of Erythrocytes and its Dependence on Medium Conductivity

The deformation of erythrocytes could only be measured with the required accuracy if the cells were kept in position at the edges of the electrodes (i.e., in the range of positive dielectrophoresis, that is between f_{d1} and f_{d2}) or attached by accident to the glass surface of the microstructures. Below f_{d1} and above f_{d2} most of the cells were repelled from the electrodes or remained freely suspended, and their deformation response could not be measured. A few cells attached by accident to the electrode or glass surfaces were slightly compressed by the field (which corresponded to a negative value of the strain $\Delta l/l_0$).

The microphotographs in Fig. 6*A–C* show the deformation response of erythrocytes suspended in a low-conductivity solution (0.11 mS cm^{-1}) and subjected to a 2-MHz field of different strengths. In accordance with the theory (*see* above), the cells showed positive dielectrophoresis (attraction to the electrode edges) associated with elongation parallel to the field (Fig. 2*B*). In some cases, the application of a field strength higher than 1.2 kV cm^{-1} led to the formation of a ''tip'' at the cell pole facing the distant electrode (Figs. 6*B* and *C*). This effect is known for erythrocytes exposed to an electric AC field [8]. Upon switching off the field, the erythrocytes elastically assumed their original shape (Fig. 6*D*).

Measurements of the relative cell elongation were performed by varying the field strength from 0.2 to 1.9 kV cm^{-1} in steps of 0.1 kV cm^{-1} at a fixed frequency of 2 MHz (Fig. 7). Curve fitting revealed a strictly quadratic dependence of the elastic strain, $\Delta l/l_0$, on the applied field strength E as predicted by Eq. 4.

Typical electrodeformation spectra of erythrocytes obtained from the evaluation of the microphotographs (illustrated in Fig. 6) are shown in Fig. 8 for different conductivities of the suspending medium. It is obvious from Figs. 6–8 that the electrodeformation response of the cells was subject to a large variability (the coefficient of variation of cell elongation was 30–60%). This variation probably originates mainly from the well-known large variation of the elastic properties [4] and, to a lesser extent, from a variation of the electric properties of the individual cells. Despite this, the deformation spectra could be fitted quite accurately on the basis of the single-shell model (combination of Eqs. 2, 3 and 4) by using the parameters extracted from the electrorotation spectra (*see* above).

In agreement with the theoretical considerations about the complex polarizability U^* (*see* also Fig. 1*A*), the cells showed negative dielectrophoresis below the crossover frequency f_{d1}. In this low-frequency range the real part of U^* is given by U_1 (Eq. 7*a*). Using appropriate values for the various cell parameters derived from electrorotation experiments it could be easily shown that U_1 was nearly independent of the external specific conductivity (as already mentioned in Theoretical Considerations). Between f_{d1} and f_{d2}, positive dielectrophoresis and, correspondingly, cell elongation parallel to the field lines was observed. Calculations of U_2 showed that at these frequencies the electromechanical stress (and thus the deformation force) depends strongly on the external specific conductivity in agreement with the theory.

It is interesting to note that the frequency-dependence of the deformation response of erythrocytes shown in Fig. 8 resembled that reported for the amoeba

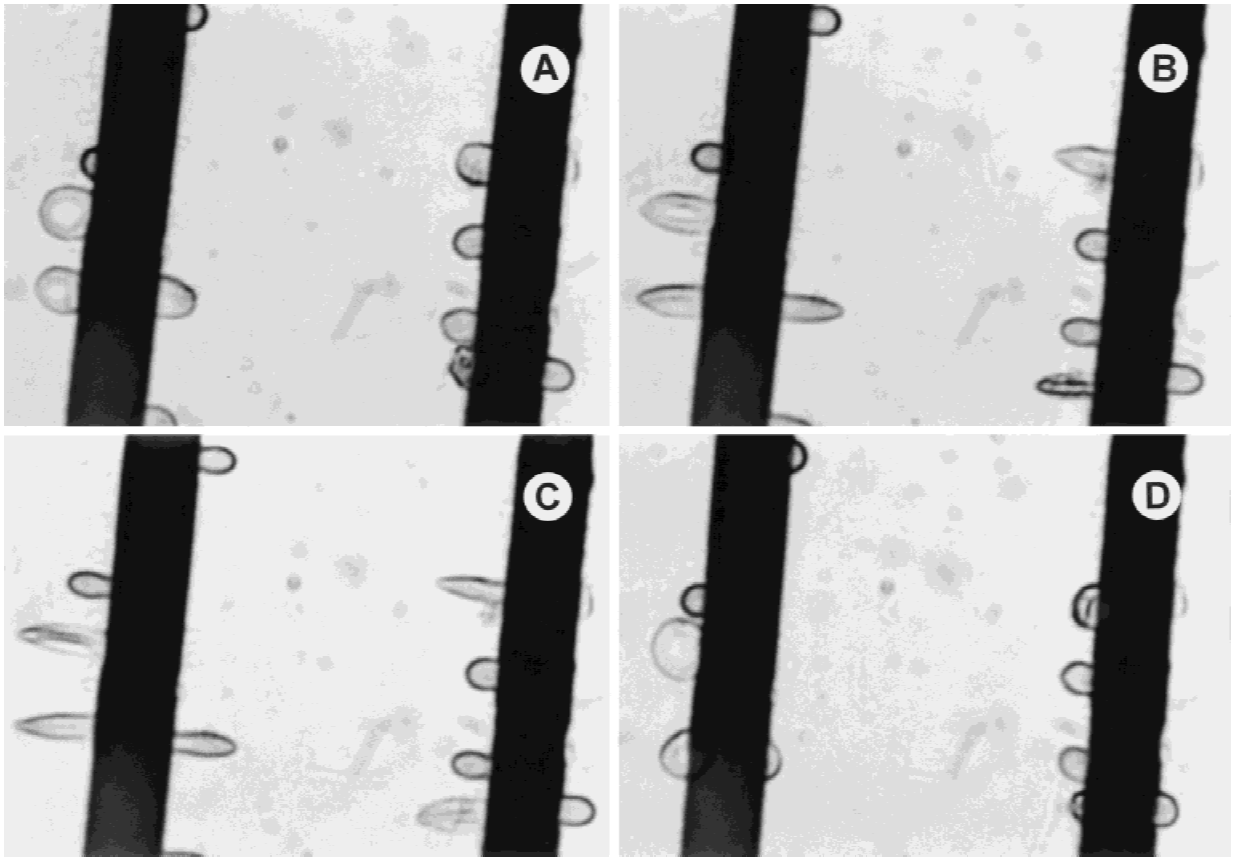

Fig. 6. Typical microphotographs of human erythrocytes exposed to an alternating current field of 2 MHz frequency and of different strengths (*A*) 0.4 kV cm^{-1}; (*B*) 1.2 kV cm^{-1}; (*C*) 1.9 kV cm^{-1}; (*D*) removal of the AC field). The experiments were performed in a low-conductivity medium (0.11 mS cm^{-1}). Note that electrodeformation (elongation parallel to the field lines) increased with increasing field strength, and that upon removal of the field the erythrocytes regained their original shape.

Chaos chaos suspended in a low–conductivity solution of 0.2 mS cm^{-1} [10]. The amoeba shows perpendicular elongation (*i.e.*, compression) at frequencies between 1 and 100 kHz, whereas higher field frequencies (up to 10 MHz) cause its elongation parallel to the field lines.

As also predicted by the theory, the crossover frequencies of electrodeformation (and dielectrophoresis) of the erythrocytes, f_{d1} and f_{d2}, corresponded roughly to the anti- and co-field frequencies f_{c1} and f_{c2} of the rotation spectra at a given medium conductivity (compare Fig. 8 with Fig. 5). Furthermore, f_{d1} shifted with increasing conductivity towards higher frequencies, whereas f_{d2} was nearly independent of σ_e. Also, the stretching of the cells between f_{d1} and f_{d2} decreased considerably with increase in the medium conductivity (Fig. 8).

Transient Deformation Forces During Electrohemolysis

The consistent description of the electrorotation-, electrodeformation- and dielectrophoresis-data on the basis of the single-shell model justified the extrapolation of the above considerations to the time domain, i.e., to the postulated role of electrodeformation forces during the DC-field-mediated electropermeabilization (Fig. 4). It is clear from the analysis of the AC-electrodeformation spectra that only the cytosolic polarization (between f_{d1} and f_{d2}) given by U_2 is strongly dependent on the external conductivity. Calculation of U_2 (relative to its value at $\sigma_e = 1$ mS cm^{-1}) as a function of the external specific conductivity (using Eq. 7*b*) yields a curve (Fig. 4) which coincided quite well with the experimental data on electrohemolysis in media of increasing conductivity. The agreement between the conductivity-dependence of U_2 and that of electrohemolysis corroborates the conclusion that the electric stress and the resulting elongation forces which arise from the transient polarization of the cytosol are predominantly responsible for the enhanced electropermeabilization of the membranes in low-conductivity media: the breakdown area is apparently enlarged by mechanical stretching of the plasma membrane under this condition.

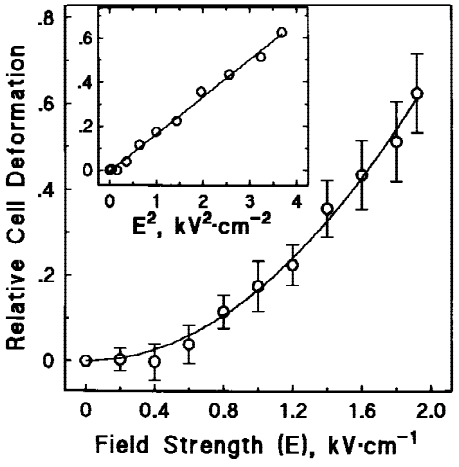

Fig. 7. Quadratic dependence of the relative cell deformation $\Delta l/l_o$ on the applied field strength E at a fixed frequency of 2 MHz. Measurements were performed in a low-conductivity medium (0.12 mS cm^{-1}, 280-mOsm inositol/phosphate buffer solution). Each symbol represents the mean ± SE from 10 independent measurements. The curve shows the best fit of the function $y = a\,x^b$ to the data with the exponent $b = 2.0 \pm 0.1$ (±SE of fitting) according to Eq. 4.

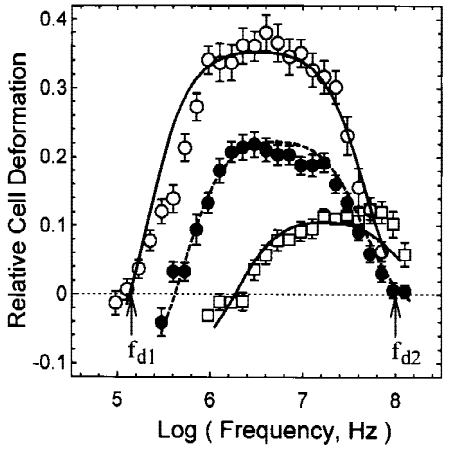

Fig. 8. Electrodeformation spectra of human erythrocytes performed in media of different conductivities: 0.11 mS cm^{-1} (open circles), 0.54 mS cm^{-1} (filled circles) and 1.95 mS cm^{-1} (squares). Datapoints are the mean ± SE of 10–12 independent measurements. The fitting curves were computed using the single-shell model (combination of Eqs. 2, 3 and 4) and the cellular parameters deduced from the rotational spectra shown in Fig. 5. Note that the crossover frequency f_{d1} (where transition from cell compression to cell elongation and simultaneously transition from negative to positive dielectrophoresis occurs) shifts towards higher frequencies with increasing medium conductivity. In contrast, the crossover frequency f_{d2} (where the conductivity-dependent cytosolic polarization disappears and, therefore, cell elongation does not occur) remains nearly unaltered.

The findings and conclusions presented here have far-reaching implications for genetic manipulations of cells by electric field techniques because chemical facilitators are conceivable which modify the deformability of the cells or which alter the dependence of electrodeformation on medium conductivity. In addition, the results can explain many conflicting data in the literature (for review, *see* [44]) because variations of the ingredients (e.g., divalent cations) of the pulse media may greatly influence the electrodeformation of the cells and thus the uptake rate of xenomolecules as well as the release of intracellular solutes.

This work was supported by grants of the DFG (Zi-99/11-1) and of the BMBF (VDI 13 MV 0305) to U.Z. The authors are grateful to G. Fuhr and Th. Schnelle for critical reading of the manuscript, for helpful discussions and for the manufacture of the microstructure electrodes.

References

1. Arnold, W.M., Zimmermann, U. 1982. Rotating-field-induced rotation and measurement of the membrane capacitance of single mesophyll cells of *Avena sativa*. *Z. Naturforsch.* **37c:**908–915
2. Arnold, W.M., Zimmermann, U. 1988. Electro-rotation: development of a technique for dielectric measurements on individual cells and particles. *J. Electrostatics* **21:**151–191
3. Becker, F.F., Wang, X.-B., Huang, Y., Pethig, R., Vykoukal, J., Gascoyne, P.R.C. 1995. Separation of human breast cancer cells from blood by differential dielectric affinity. *Proc. Natl. Acad. Sci. USA* **92:**860–864
4. Brody, J.P., Han, Y., Austin, R.H., Bitensky, M. 1995. Deformation and flow of red blood cells in a synthetic lattice: Evidence for an active cytoskeleton. *Biophys. J.* **68:**2224–2232
5. Bryant, G., Wolfe, J. 1987. Electromechanical stresses produced in the plasma membranes of suspended cells by applied electric fields. *J. Membrane Biol.* **96:**129–139
6. Djuzenova, C.S., Zimmermann, U., Frank, H., Sukhorukov, V.L., Richter, E., Fuhr, G. 1996. Effect of medium conductivity and composition on the uptake of propidium iodide into electropermeabilized myeloma cells. *Biochim. Biophys. Acta* **1284:**143–152
7. Doetsch, G. 1967. Anleitung zum Praktischen Gebrauch der Laplace-Transformation und der Z-Transformation. R. Oldenbourg Verlag, München
8. Engelhardt, H., Sackmann, E. 1988. On the measurement of shear elastic moduli and viscosities of erythrocyte plasma membranes by transient deformation in high frequency electric fields. *Biophys. J.* **54:**495–508
9. Engelhardt, H., Gaub, H., Sackmann, E. 1984. Viscoelastic properties of erythrocyte membranes in high-frequency electric fields. *Nature* **307:**378–380
10. Friend, A.W., Finch, E.D., Schwan, H.P. 1975. Low frequency electric field induced changes in the shape and mobility of amoebas. *Science* **187:**357–359
11. Fuhr, G., Kuzmin, P.I. 1986. Behavior of cells in rotating electric fields with account to surface charges and cell structures. *Biophys. J.* **50:**789–795
12. Fuhr, G., Zimmermann, U., Shirley, S.G. 1996. Cell motion in time-varying fields: Principles and potential. *In:* Electromanipulation of Cells. U. Zimmermann and G.A. Neil, editors. pp. 259–328. CRC Press, Boca Raton, FL
13. Gascoyne, P.R.C., Becker, F.F., Wang, X.-B. 1995. Numerical analysis of the influence of experimental conditions on the accuracy of dielectric parameters derived from electrorotation measurements. *Bioelectrochem. Bioenerg.* **36:**115–125

14. Gauger, B., Bentrup, F.-W. 1979. A study of dielectric membrane breakdown in the *Fucus* egg. *J. Membrane Biol.* **48:**249–264
15. Gimsa, J., Marszalek, P., Loewe, U., Tsong, T.Y. 1991. Dielectrophoresis and electrorotation of neurospora slime and murine myeloma cells. *Biophys. J.* **60:**749–760
16. Gimsa, J., Müller, T., Schnelle, T., Fuhr, G. 1996. Dielectric spectroscopy of single human erythrocytes at physiological ionic strength: Dispersion of the cytoplasm. *Biophys. J.* **71:**498–506
17. Glaser, R., Fuhr, G., Gimsa, J. 1983. Rotation of erythrocytes, plant cells, and protoplasts in an outside rotating electric field. *Studia biophysica* **96:**11–20
18. Haest, C.W.M., Kamp, D., Deuticke, B. 1997. Transbilayer reorientation of phospholipid probes in the human erythrocyte membrane. Lessons from studies on electroporated and resealed cells. *Biochim. Biophys. Acta* **1325:**17–33
19. Helfrich, W. 1974. Deformation of lipid bilayer spheres by electric fields. *Z. Naturforsch.* **29c:**182–183
20. Henszen, M.M.M., Weske, M., Schwarz, S., Haest, C.W.M., Deuticke, B. 1997. Electric field pulses induce reversible shape transformation of human erythrocytes. *Mol. Membr. Biol.* **14:**195–204
21. Holzapfel, C., Vienken, J., Zimmermann, U. 1982. Rotation of cells in an alternating electric field: Theory and experimental proof. *J. Membrane Biol.* **67:**13–26
22. Jeltsch, E., Zimmermann, U. 1979. Particles in a homogeneous electrical field: A model for the electrical breakdown of living cells in a Coulter counter. *Bioelectrochem. Bioenerg.* **6:**349–384
23. Jones, T.B. 1995. Electromechanics of Particles, Cambridge University Press, New York
24. Kinosita, K., Tsong, T.Y. 1977. Formation and resealing of pores of controlled sizes in human erythrocyte membrane. *Nature* **268:**438–441
25. Lynch, P.T., Davey, M.R. 1996. Electrical Manipulation of Cells, Chapman & Hall, New York
26. Mahaworasilpa, T.L., Coster, H.G.L., George, E.P. 1996. Forces on biological cells due to applied alternating (AC) electric fields. II. Electro-rotation. *Biochim. Biophys. Acta* **1281:**5–14
27. Pastushenko, V.Ph., Kuzmin, P.I., Chizmadzhev, Yu.A. 1985. Dielectrophoresis and electrorotation — a unified theory of spherically symmetrical cells. *Studia biophysica* **110:**51–57
28. Pauly, H., Schwan, H.P. 1959. Über die Impedanz einer Suspension von kugelförmigen Teilchen mit einer Schale. Ein Modell für das dielektrische Verhalten von Zellsuspensionen und von Proteinlösungen. *Z. Naturforsch.* **14b:**125–131
29. Pawlowski, P., Fikus, M. 1989. Bioelectroreological model of the cell. I. Analysis of stresses and deformations. *J. Theor. Biol.* **137:** 321–337
30. Pethig, R., Kell, D.B. 1987. The passive electrical properties of biological systems: the significance in physiology, biophysics and biotechnology. *Phys. Med. Biol.* **32:**933–977
31. Popov, S.V., Svitkina, T.M., Margolis, L.B., Tsong, T.Y. 1991. Mechanism of cell protrusion formation in electrical field: The role of actin. *Biochim. Biophys. Acta* **1066:**151–158
32. Scheurich, P., Zimmermann, U. 1980. Membrane fusion and deformation of red blood cells by electric fields. *Z. Naturforsch.* **35c:**1081–1085
33. Stenger, D.A., Kaler, K.V.I.S., Hui, S.W. 1991. Dipole interactions in electrofusion. Contribution of membrane potential and effective dipole interaction pressures. *Biophys. J.* **59:**1074–1084
34. Sukhorukov, V.L., Arnold, W.M., Zimmermann, U. 1993. Hypotonically induced changes in the plasma membrane of cultured mammalian cells. *J. Membrane Biol.* **132:**27–40
35. Sukhorukov, V.L., Zimmermann, U. 1996. Electrorotation of erythrocytes treated with dipicrylamine: Mobile charges within the membrane show their ''signature'' in rotational spectra. *J. Membrane Biol.* **153:**161–169
36. Winterhalter, M., Helfrich, W. 1988. Deformation of spherical vesicles by electric fields. *J. Colloid Interf. Sci.* **122:**583–586
37. Wolfram, S. 1996. The *Mathematica*® Book. Third Edition. Wolfram Media, Champain, IL
38. Zimmermann, U. 1982. Electric field-mediated fusion and related electrical phenomena. *Biochim. Biophys. Acta* **694:**227–277
39. Zimmermann, U., Neil, G.A. 1996. Electromanipulation of Cells, CRC Press, Boca Raton, FL